Fine-Tuning the Synthesis of ZnO Nanostructures by an Alcohol Thermal Process

J. P. Cheng,* X. B. Zhang, X. Y. Tao, H. M. Lu, Z. Q. Luo, and F. Liu*

Department of Materials Science and Engineering, State Key Laboratory of Silicon Materials, Zhejiang University, Hangzhou 310027, People's Republic of China

Received: January 8, 2006; In Final Form: March 20, 2006

A simple and efficient alcohol thermal technique was applied to control the growth of the dimensions and morphology of ZnO nanostructures under mild conditions, where surfactant was not necessary. The size of ZnO nanocrystals increased with growth temperature and they transformed into nanorods with different aspect ratios through tuning the reaction time. The length of nanorods increased significantly with the reaction time, but their thickness only slightly increased. The as-prepared ZnO nanocrystals were monocrystalline and the growth orientation of ZnO nanorods was [001]. Photoluminescence measurements showed a blue shift in violet emission with a reduction in crystal size and revealed the quantum confinement effect. Electron irradiation induced structural damage was observed in the ZnO nanorods synthesized at 120 °C. Experimental results proved that the possible growth mechanism of ZnO nanostructures was oriented attachment.

Introduction

Semiconductive oxide ZnO is an important material for applications in many fields. ZnO nanocrystals have increased the interest in the use of this material for short wavelength light emitters and transparent electronics.[1] ZnO crystals with different configurations, such as nanorods (nanowires),[2] nanoparticles,[3] nanoribbons,[4] tetrapods,[5] and towerlike,[6] tubelike,[6,7] and flowerlike ZnO[6,8] have been successfully fabricated. Most techniques to fabricate ZnO nanostructures, such as vapor phase transport deposition,[1,5] chemical vapor deposition,[4] pulsed laser ablation,[9] electrodeposition,[10] ultrasonic irradiation,[3] and thermal evaporation,[11] are not suitable for controllable synthesis; in addition to being complex processes, sophisticated equipment and economically prohibitive high temperatures are required.

Chemical methods, such as sol−gel,[6,12] template growth,[7,13] and hydrothermal methods,[8,14] have been proved to be attractive due to the low growth temperature and easy operation, promising scale-up fabrication. However, these chemical methods yield either a mixture of different morphologies of ZnO structures with a larger size or extremely small nanocrystals, with little control over a wide range.[3,12] To obtain a controllable synthesis of ZnO nanocrystals, some additives such as surfactant or complexing agent are extensively applied in the reaction process.[8,14,15]

Recently, much effort has been made in controlling the size and morphology of ZnO nanostructures.[2,3,15] Challenges, however, still remain. These include, for instance, achieving further reductions in crystal size, improving control of the crystal morphology, and gaining a deeper understanding of the growth mechanism. In this paper, we describe an alcohol thermal method to prepare different morphologies of ZnO nanostructures through adjusting the growth temperature and reaction time, wherein no surfactants are involved. A possible growth mechanism is proposed on the experimental results.

* Corresponding authors. Tel./fax: +86-571-87951411. E-mail: mseem@zju.edu.cn.

Experimental Section

Fabrication of ZnO Nanocrystals. The preparation procedure described by Meulenkamp[16] has been developed by Qian et al. to synthesize monodispersed ZnO nanocrystals with a size smaller than 7 nm.[3] Different from Qian's ultrasonic irradiation process,[3] alcohol thermal treatment is employed in our cases to fabricate ZnO nanoparticles and nanorods in a large size range.

All chemicals were analytical grade reagents and purchased from commercial sources without further treatment. In a typical procedure, 2.4 g of $Zn(Ac)_2 \cdot 2H_2O$ was added into 60 mL of absolute alcohol and then the solution was under magnetic stirring at 0 °C for hours to form a Zn-containing suspension. Separately, 1.0 g of $LiOH \cdot H_2O$ was added into 60 mL of anhydrous alcohol at room temperature. The Li-containing solution was added into the Zn-containing suspension dropwise at 0 °C under stirring. The resultant mixture was then loaded into a Teflon-lined autoclave with a filling capacity of about 80%. The sealed autoclave was maintained at 90−150 °C for 2−10 h. After cooling to room temperature naturally, white precipitate was collected and washed with distilled water and alcohol several times to obtain ZnO nanocrystals.

Meulenkamp had suggested that the precursor of the reaction was basic zinc−lithium acetate during the nucleation, and the conversion of the precursor to ZnO nanocrystallites was very slow at 0 °C.[16] The dissolved species during the growth is not known yet and acetate is a good complexant for Zn^{2+}. Oxides can be formed by hydrolysis (eq 1) and condensation (eq 2) of the dissolved species[16]

$$\mathrm{Zn{-}OAc + HOH/OH^- \Leftrightarrow Zn{-}OH + HOAc/OAc^-} \quad (1)$$

$$\mathrm{Zn{-}OH + Zn{-}OAc \Leftrightarrow Zn{-}O{-}Zn + HOAc} \quad (2)$$

where the dissolved species is denoted as Zn−OAc.

Characterization Methods. Powder samples were used for the structural measurements by X-ray powder diffraction (XRD, D/max-rA) with Cu Kα radiation. The size and morphology of ZnO nanocrystals were observed with a scanning electron

10.1021/jp060133s CCC: $33.50
Published on Web 05/10/2006

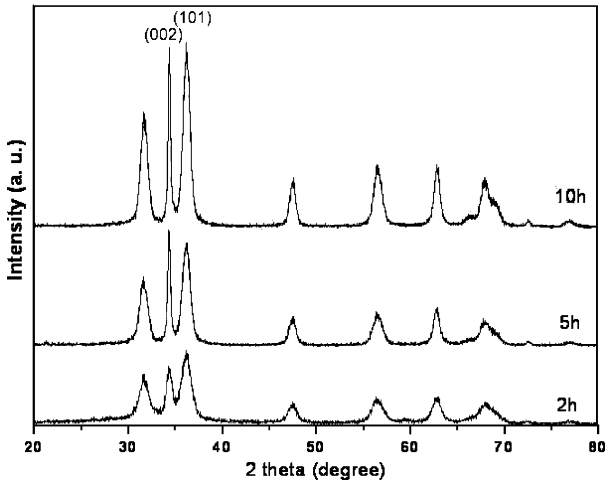

Figure 1. XRD patterns of ZnO samples fabricated at 120 °C for different reaction times.

microscope (SEM, FEI sirion) and transmission electron microscope (TEM, JEOL-2010) with an attached energy-dispersive X-ray spectrometer (EDS). Photoluminescence (PL) spectra of ZnO nanocrystals were measured with a Hitachi F-4500 fluorescence spectrophotometer using a Xe lamp with an excitation wavelength of 325 nm at room temperature.

Results and Discussion

Characterization of Products. The crystallinity of ZnO samples was investigated through XRD analysis. Figure 1 shows XRD patterns of the samples fabricated at 120 °C for 2, 5, and 10 h, respectively. The crystallographic phases of samples are all in good agreement with the JCPDS card (no. 36-1451) for the typical wurtzite-type ZnO crystal. The full width of the (002) peak at half-maximum is narrowest in all peaks in a single profile. The remarkable difference in the full width at half-maximum supports our inference that ZnO crystals may promote along the [001] direction, resulting in the formation of nanorods.[17] However, All the diffraction peaks are broadening, suggesting that these products should exhibit a small crystal size. The crystallite size (D_{XRD}) is determined using the diffraction peak of the (101) ZnO plane ($2\theta = 36.2°$) and Scherrer equation [$D_{XRD} = 0.9\lambda/(\beta \cos \theta)$,[18] where λ is the characteristic wavelength of the X-ray used, θ the diffraction angle, and β the angular width in radians at an intensity equal to half of the maximum peak intensity]. The crystal size D_{XRD} is estimated to be 8 nm for 2 h synthesis, 10 nm for 5 h, and 11 nm for 10 h. This implies that the ZnO crystal is coarsening with reaction time and our subsequent TEM observations also prove it.

The crystal size and morphology of ZnO fabricated at 120 °C have been studied with TEM. The ZnO sample fabricated for 2 h is shown in parts a and b of Figure 2, where the crystals exhibit as agglomerated nanoparticles with a small size distribution, from 8 to 10 nm. A typical high-resolution TEM (HRTEM) image in Figure 2b proves that these nanoparticles are monocrystalline in nature. From the lattice fringes, it is seen that these particles are approximately spherical and that many particles exhibit some facets. As the reaction time is prolonged to 5 h,

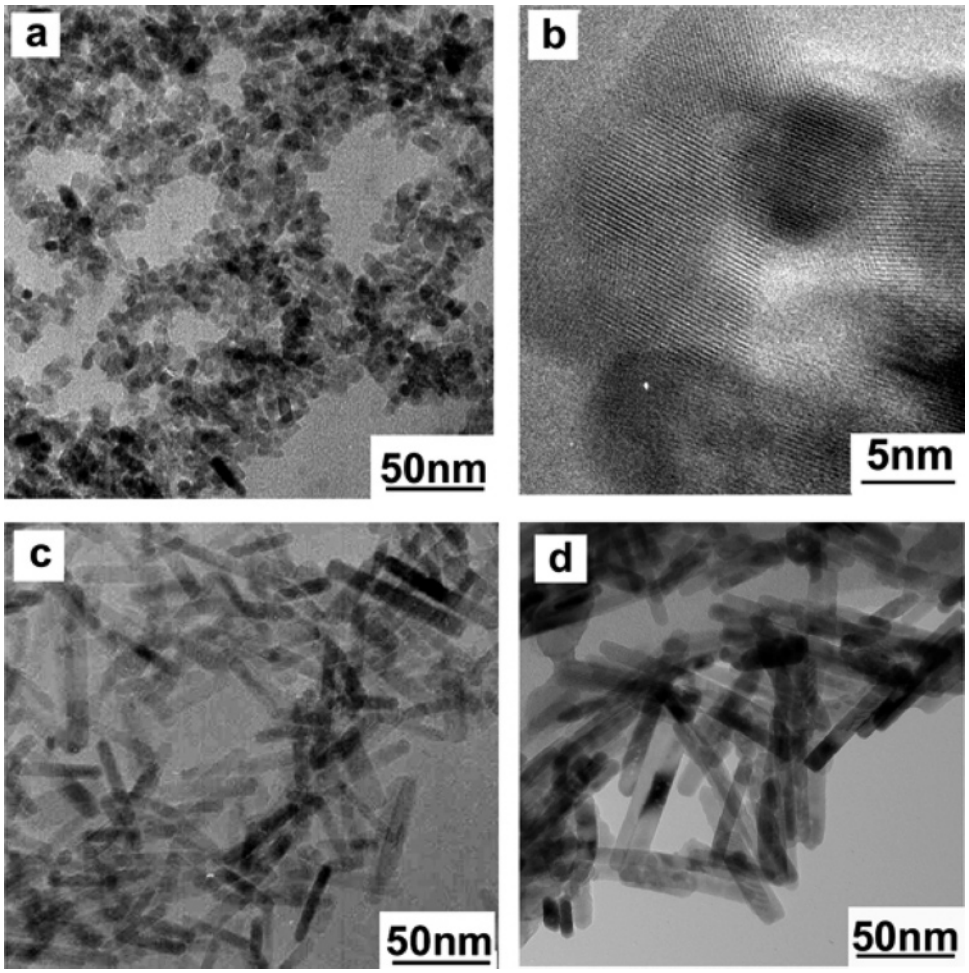

Figure 2. TEM images of ZnO samples fabricated at 120 °C for different times: (a, b) 2 h, (c) 5 h, and (d) 10 h.

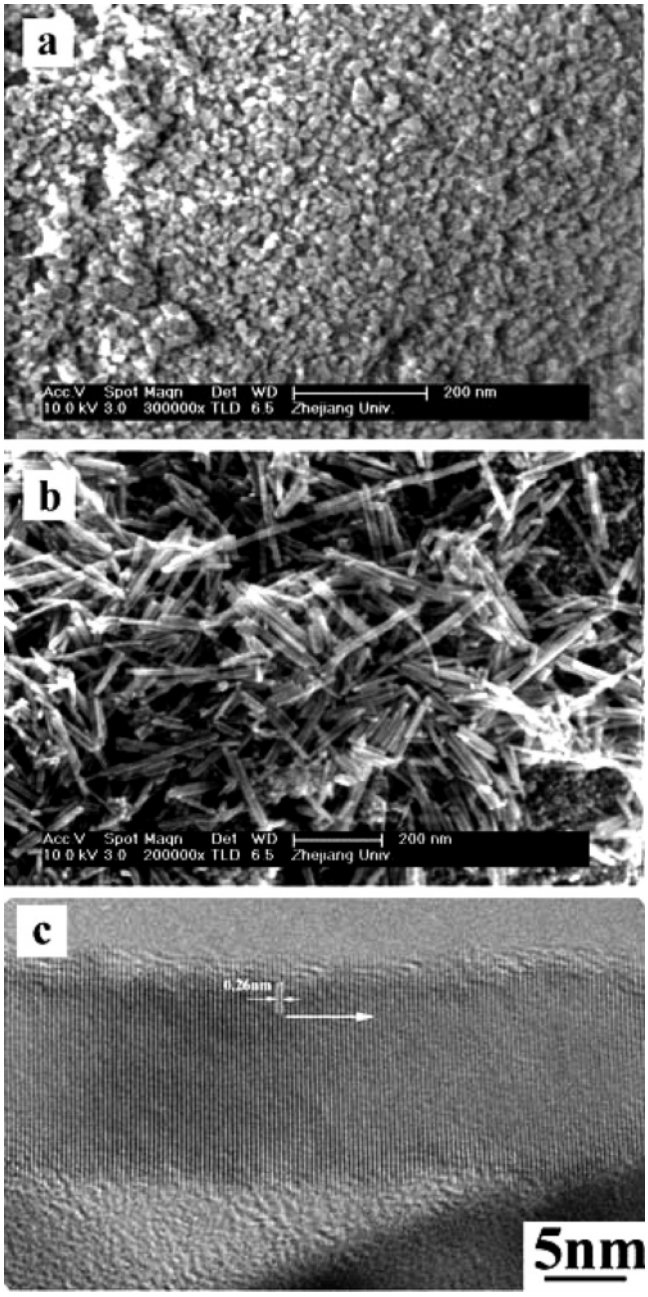

Figure 3. SEM and HRTEM images of ZnO crystals fabricated at 150 °C for (a) 2 h and (b, c) 10 h.

the morphology of crystals is elongated to form nanorods in Figure 2c, whose diameter is comparable to that of nanoparticles and the aspect ratio value is lower than 7. For the sample prepared for 10 h, a large fraction of ZnO nanorods with aspect ratio values higher than 10 is formed in Figure 2d. However, the diameter of ZnO nanorods is restricted within a narrow limit and only increased slightly. From TEM observations, it is reasonable to deduce that the rodlike ZnO crystals are originated from ZnO nanoparticles. Because their diameter is similar, these nanorods should have grown in a preferential growth orientation. So the length of ZnO nanorods is strongly correlated with reaction time, an increase of reaction time mainly leading to an elongation of crystals, suggesting a controllable synthesis. This result implies that the aspect ratio of ZnO nanorods can be easily modulated with reaction time.[17]

The SEM images of ZnO samples prepared at 150 °C are shown in Figure 3. The ZnO product contains a large number of particles with an average size of 15 nm (Figure 3a), when

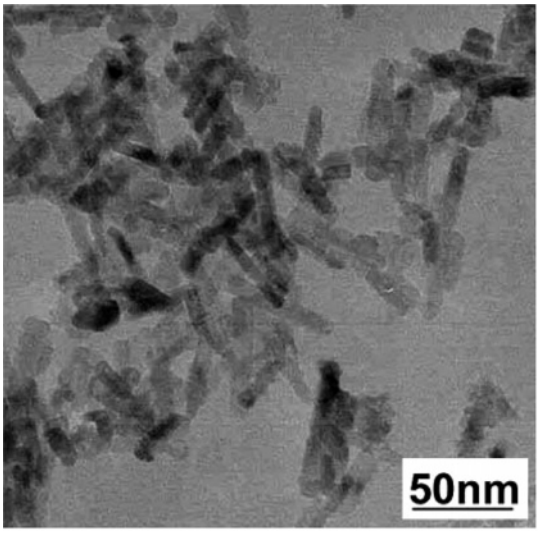

Figure 4. A typical TEM image of ZnO fabricated at 90 °C for 10 h.

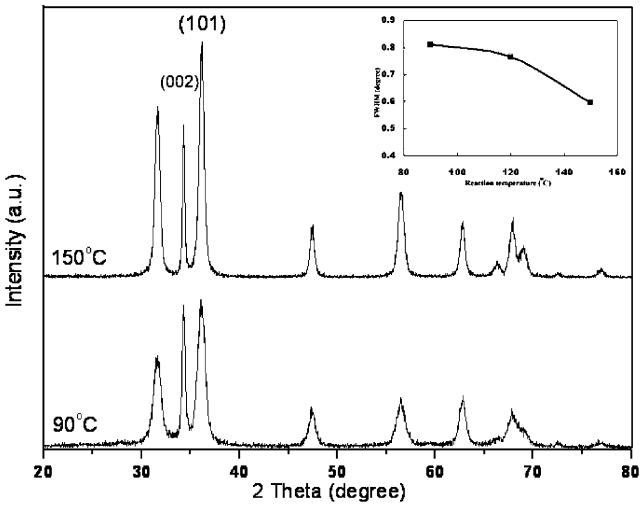

Figure 5. XRD patterns of ZnO fabricated at 90 and 150 °C for 10 h. Inset: the relationship between growth temperature and fwhm value of (101) peaks.

the reaction time is set for 2 h. Similar to those synthesized at 120 °C, ZnO nanorods with uniform diameter are obtained for 10 h growth, as shown in Figure 3b. The mean diameter of these nanorods is also about 15 nm. Figure 3c shows an HRTEM image corresponding to the sample in Figure 3b. It clearly shows a well-resolved lattice with a measured interplane spacing of 0.26 nm, consistent with the distance between (002) crystal planes. HRTEM observations suggest that the preferred growth direction of nanorods is parallel to the [001] crystallographic direction (*c*-axis), indicated with an arrow in Figure 3c. The rough surface of the nanorod in Figure 3c implies that a large amount of surface defects exists on the surface.

As the growth temperature was fixed at 90 °C, we still got very similar results. Much smaller ZnO particles were obtained for 2 h synthesis. The length of ZnO crystals increased considerably with increasing reaction time, but their diameter was strictly limited. Figure 4 presents a typical TEM image of ZnO nanocrystals fabricated at 90 °C for 10 h. It shows that the diameter of the formed ZnO nanorods is much small, i.e. about 7 nm.

Figure 5 shows XRD patterns of ZnO products fabricated at 90 and 150 °C for 10 h, respectively. They have similar profile and all diffraction peaks can be indexed as the crystalline ZnO with the hexagonal wurtzite structure. No peaks of any impuri-

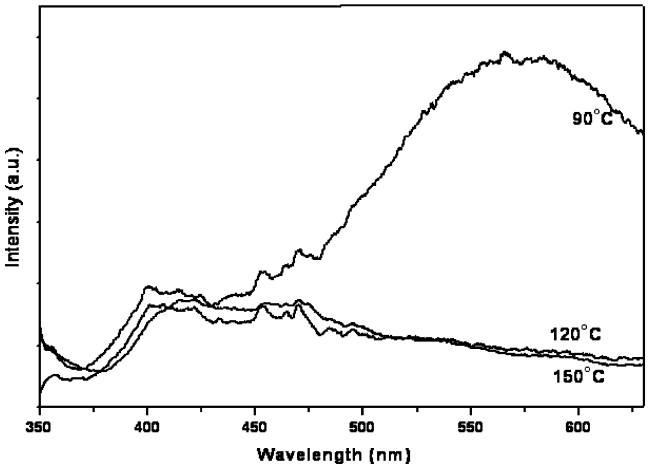

Figure 6. Room-temperature PL spectra recorded from ZnO nanorods grown for 10 h at different temperatures, showing a blue shift in violet emission with a reduction in crystal size.

ties are detected in the patterns. The relative sharpened (002) peaks imply that they transform into nanorods in the [001] direction, consistent with TEM observations. Even if fabricated at 90 °C, a relative low temperature, ZnO nanostructures still remain crystalline. To further understand the relationship between the crystal size and growth temperature, the dependence of fwhm (full width at half-maximum) values of the (101) peak on the growth temperature is shown in the inset of Figure 5. It can be clearly seen that the fwhm values decrease monotonically as the growth temperatures increase, i.e. the size of ZnO crystals increases with increasing temperature, which is consistent with TEM observations. So the crystal size of ZnO is closely dependent on the growth temperature.[19] We can thus obtain various ZnO nanoparticles and nanorods with uniform size and diameter by controlling the growth temperature.

Photoluminescence Measurements. To characterize the optical properties of as-prepared ZnO nanocrystals, photoluminescence spectra of ZnO nanorods were measured at room temperature. Figure 6 shows the photoluminescence spectra of ZnO nanorods synthesized at different temperatures. Three emitting bands, including a violet emission at around 400−420 nm, a blue band at about 450−470 nm, and a green band at about 550 nm are observed. This is considerably different from the typical observation in ZnO crystals, which usually exhibit a narrow UV peak at 370−390 nm and a broad green emission at 510−550 nm.[20] For the violet emission, they may be due to radiative defects related to the interface traps existing at the grain boundaries and emitted from the radiative transition between this level and the valence band.[21] The blue-band emission may originate from the recombination of oxygen vacancies with oxygen interstitials or other defects.[22] The exact mechanisms for violet and blue emissions are not yet clear to us. It has been suggested that the green emission peaks at about 550 nm correspond to the singly ionized oxygen vacancy in ZnO and result from the recombination of a photogenerated hole with the singly ionized charge state of this defect.[23] The progressive increase of the green emission as the rod diameter decreases suggests that there is a great fraction of oxygen vacancies in the thinner nanorods. A higher surface area to volume ratio for thinner nanorods will favor a higher level of surface and subsurface oxygen vacancy.[5] EDS analyses demonstrate that the atomic ratios of Zn to oxygen in ZnO nanocrystals fabricated at 90, 120, and 150 °C are about 1.17, 1.08, and 1.06, respectively, which are generally consistent with

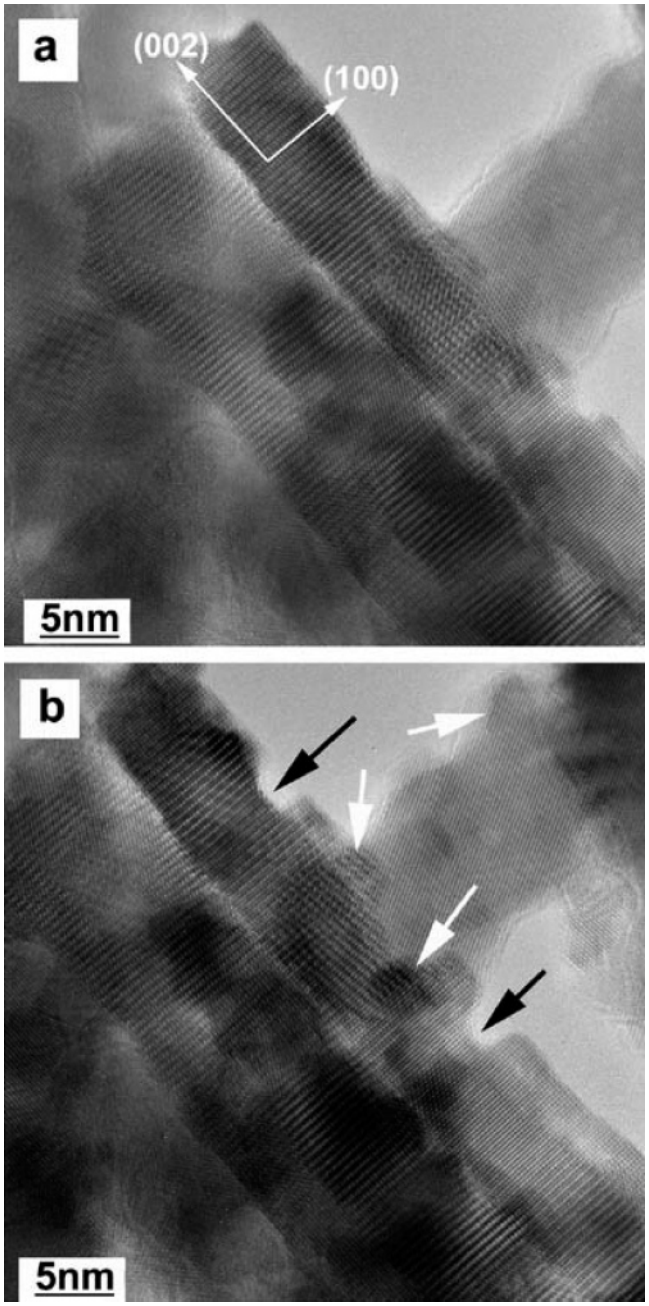

Figure 7. HRTEM images of ZnO nanorods under irradiation of 200 kV electron beam: (a) initiation state and (b) after 3 min of irradiation.

above discussion. In this regard, different temperatures and sizes cause different point defect densities in crystals.

The difference of PL properties between the present ZnO nanorods and the previous reports[9,20] may be caused by the lattice defects during the low-temperature synthesis process. It is found that the violet emission peaks give rise to a blue shift from 414 to 398 nm with the decrease of growth temperature. It should be caused by a reduction in particle size, because quantum confinement generally shifts the energy levels of the conduction and valence bands apart, giving rise to a blue shift in the transition energy as the particle size decrease.[12,23,24]

Microstructure Analyses. From PL measurements, we speculated that as-prepared ZnO nanorods should be of a high density of point defects that was hardly detected by HRTEM observations. Here we find a very interesting phenomenon, electron irradiation induced structural damage in ZnO nanocrystals, and it is revealed in Figure 7. Figure 7a presents an

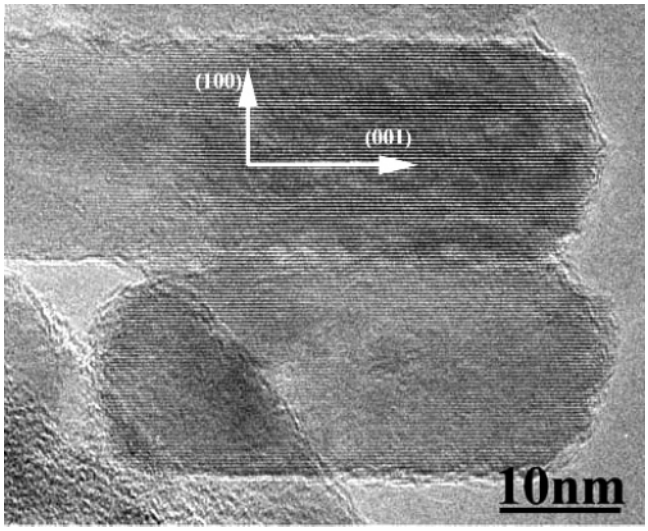

Figure 8. An HRTEM image showing the aggregated ZnO nanorods.

HRTEM image of several ZnO nanorods fabricated at 120 °C for 10 h in which these nanorods are grown along [001] direction from lattice spacing measurement. The structural damage in ZnO nanocrystals is demonstrated in Figure 7b after irradiation for 3 min with 200 kV electrons. Comparing two HRTEM images, some remarkable changes in morphology are observed. ZnO nanorods exposed to electron irradiation look damaged, for their initial surface is destroyed and some concave facets are left, as pointed out with black arrows in the micrograph. At the same time, some newly developed nanocrystals indicated with white arrows are observed close to the damage sites. Susceptibility to electron beam damage leads to a difficulty in determining the structural relation between the resultant crystals and their precursors. In addition to PL spectra, perhaps this is also evidence that a considerable density of point defects, such as oxygen vacancies, exist in the as-prepared nanorods, because materials with large amount of point defects are sensitive to the electron irradiation.

From observed structural damage under electron irradiation, we infer that these nanorods are composed of ZnO nanocrystals with extremely small size, similarly to previous reports.[7,25] On the contrary to these polycrystalline nanorods,[7,25] ZnO rods in our cases are monocrystalline. Pacholski and co-workers revealed that preformed quasispherical ZnO nanoparticles tended to aggregate to form single crystalline rodlike particles by evaporation of methanol solvent.[26] In ZnO nanorods fabricated at 150 °C, we find similar aggregated nanorods. Figure 8 shows an oriented attachment between two nanorods parallel to the *c*-axis of crystals. It can be seen that the depicted particles are perfect and stable under electron irradiation. They parallel align and the lattice planes go straight through the contact area without dislocation. These imply that ZnO nanorods are better crystallized at 150 °C than at 120 °C and that large ZnO crystals may be built by oriented coalescing.

Growth Mechanism. These days, several mechanisms have been proposed to interpret the growth of one-dimensional crystalline nanosized structures, for instance the VLS[27] and the VS[28] processes. In the present synthesis, there are no external catalysts and surfactant introduced. It is clear that ZnO nanorods in our cases are grown neither by the VS nor the VLS growth mechanism. However, our experimental results also provide a number of insights into the likely growth mechanism. Nearly monodispersed small ZnO nanoparticles obtained by simply hydrolyzing zinc acetate in alcohol solution were studied two decades ago.[3,16,29−31] A rapid formation of extremely small ZnO particles in alcohol was followed by a relatively slow growth of the particles. When the alcohol suspension was aged at room temperature, it took several days for the particles to attain their final size.[16,30−31] The rate of particle growth depended strongly on the growth temperature.[16]

In our cases, the growth process of alcoholic ZnO colloid was never assisted by organic ligand or by solution evaporation.[26,31−33] Preformed ZnO building units could move freely in the solution. To decrease the high surface energy, the adjacent particles would be self-assembled and oriented by attach one-by-one toward the formation of large crystals. Pacholski et al.[26] have offered strong evidence that oriented attachment of preformed quasispherical ZnO nanoparticles was a major reaction path during the formation of single crystalline nanorods. The bottlenecks between adjacent particles should have been filled up and the surface of resultant nanorods must have been smoothened along the *c*-axis in the growth process. If some local filling areas are imperfect in crystallization, the formed nanorods will be metastable and result in recrystallization under electron irradiation, as shown in Figure 7. For the as-prepared ZnO nanocrystals, the chemical component of ZnO nanorods is nonstoichiometric and usually consists of excess Zn atoms and oxygen vacancies. Therefore, lattice defects and surface defects are contained in the as-grown ZnO crystals. Some crystal imperfections, such as point defects, dislocations, and grain boundaries will be appeared and further study is underway. The oriented coalescing of nanorods in Figure 8 is also observed by Liu B et al.,[34] i.e. the side crystal planes gluing together to form a larger crystal. Li Q et al. even observed that some ZnO nanorods were formed out of bundling of smaller diameter nanorods.[19] All these suggest that the likely growth mechanism in our synthesis process is oriented attachment, which is chiefly related to the intrinsic crystal structure of ZnO, as well as different growth rates of crystal faces.[2] Moreover, Meulenkamp found that the concentration of water in the reaction solution was of paramount importance and that 1.0 vol % water introduction could not lead to ZnO formation.[16] In our cases, ZnO nanocrystals still formed at 150 °C with 1.0 vol % water in the mixture due to a relative high growth temperature.

Conclusion

In summary, an alcohol thermal process is developed for the fine-tuned syntheses of ZnO nanoparticles and nanorods at mild temperature, where no surfactant is necessary. The process is well-repeatable, easily carried out, low-cost, and less hazardous. The diameter and length of ZnO nanorods can be adjusted by growth temperature and reaction time. The crystallinity of ZnO nanorods is influenced by growth temperature. Photoluminescence measurements show a blue shift in violet emission due to the quantum confinement effect. The growth mechanism of nanorods is possibly oriented attachment of preformed ZnO nanocrystals.

Acknowledgment. The authors gratefully acknowledge the financial support from National Natural Science Foundation of China (no. 50571087), and this project is supported by China Postdoctoral Science Foundation (no. 2005038621).

Supporting Information Available: Figures showing a HRTEM image of aggregated particles at the intitial state of "attachment", an example where misorientation is presented in a rod, and a typical nanorod with a rough surface. This material is available free of charge via the Internet at http://pubs.acs.org.

References and Notes

(1) Huang, M. H.; Mao, S.; Feick, H.; Yan, H. Q.; Wu, Y. Y.; Kind, H.; Weber, E.; Russo, R.; Yang, P. *Science* **2001**, *292*, 1897.

(2) Cheng, B.; Samulski, E. T. *Chem. Commun.* **2004**, 986.
(3) Qian, D.; Jiang, J. Z.; Hansen, P. L. *Chem. Commun.* **2003**, 1078.
(4) Gao, P. M.; Ding, Y.; Mai, W. J.; Hughes, W. L.; Lao, C. S.; Wang, Z. L. *Science* **2005**, *309*, 1700.
(5) Yang, P.; Yan, H. Q.; Mao, S.; Russo, R.; Johnson, J.; Saykally, R.; Morris, N.; Pham, J.; He, R.; Choi, H. J. *Adv. Funct. Mater.* **2002**, *12*, 323.
(6) Wang, Z.; Qian, X. F.; Yin, J.; Zhu, Z. K. *Langmuir* **2004**, *20*, 3441.
(7) Shen, X. P.; Yuan, A. H.; Hu, Y. M.; Jiang, Y.; Xu, Z.; Hu, Z. *Nanotechnology* **2005**, *16*, 2039.
(8) Zhang, H.; Yang, D. R.; Ji, Y. J.; Ma, X. Y.; Xu, J.; Que, D. L. *J. Phys. Chem. B* **2004**, *108*, 3955.
(9) Sun, Y.; Fuge, G. M.; Ashfold, M. N. R. *Chem. Phys. Lett.* **2004**, *396*, 21.
(10) Cao, B. Q.; Cai, W. P.; Duan, G. T.; Li, Y.; Zhao, Q.; Yu, D. P. *Nanotechnology* **2005**, *16*, 2567.
(11) Pan, Z. W.; Dai, Z. R.; Wang, Z. L. *Science* **2001**, *291*, 1947.
(12) Lin, K. F.; Cheng, H. M.; Hsu, H. C.; Lin, L. J.; Hsieh, W. F. *Chem. Phys. Lett.* **2005**, *409*, 208.
(13) Zhang, X. H.; Xie, S. Y.; Zhang, Z. Y.; Tian, Z. Q.; Xie, Z. X.; Huang, R. B.; Zheng, L. S. *J. Phys. Chem. B* **2003**, *107*, 10114.
(14) Tao, X. Y.; Zhang, X. B.; Kong, F. Z.; Lin, S.; Cheng, J. P.; Huang, W. Z.; Li, Y.; Liu, F.; Xu, G. L. *Acta Chim. Sinica* **2004**, *62*, 1658.
(15) Wang, C. L.; Shen, E. H.; Wang, E. B.; Cao, L.; Kang, Z. K.; Tian, C. G.; Lan, Y.; Zhang, C. *Mater. Lett.* **2005**, *59*, 2867.
(16) Meulenkamp, E. A. *J. Phys. Chem. B* **1998**, *102*, 5566.
(17) Lo, B.; Chang, J. Y.; Ghule, A. V.; Tzing, S. H.; Ling, Y. C. *Scrip. Mater.* **2006**, *54*, 411.
(18) Cheng, J. P.; Zhang, X. B.; Ye, Y. *J. Solid State Chem.* **2006**, *179*, 91.
(19) Li, Q.; Kumar, V.; Li, Y.; Zhang, H.; Marks, T. J.; Chang, R. P. H. *Chem. Mater.* **2005**, *17*, 1001.
(20) Cheng, J. P.; Zhang, X. B.; Luo, Z. Q. *Physica E* **2006**, *31*, 235.
(21) Wang, Q. P.; Zhang, D. H.; Xue, Z. Y.; Hao, X. T. *Appl. Surf. Sci.* **2002**, *201*, 123.
(22) Mahamuni, S.; Borgohain, K.; Bendre, B. S.; Leppert, V. J.; Risbud, S. H. *J. Appl. Phys.* **1999**, *85*, 2861.
(23) Wang, Z. L. *J. Phys.: Condens. Matter* **2004**, *16*, R829.
(24) Kamat P. V.; Patrick, B. *J. Phys. Chem.* **1992**, *96*, 6829.
(25) Yang, L.; Wang, G. Z.; Tang, C. J.; Wang, H. Q.; Zhang, L. D. *Chem. Phys. Lett.* **2005**, *409*, 337.
(26) Pacholski, C.; Kornowski, A.; Weller, H. *Angew. Chem., Int. Ed.* **2002**, *41*, 1188.
(27) (a) Cheng, J. P.; Zhang, X. B.; Ye, Y.; Tu, J. P.; Liu, F.; Tao, X. Y.; Geise, H. J.; Tendeloo, G. V. *Microporous Mesoporous Mater.* **2005**, *81*, 73. (b) Cheng, J. P.; Zhang, X. B.; Tu, J. P.; Liu, F.; Ye, Y.; Ji, Y. J.; Chen, C. P. *Carbon* **2003**, *41*, 1965.
(28) Zhang, X. H.; Zhang, Y.; Xu, J.; Wang, Z.; Chen, X. H.; Yu, D. P.; Zhang, P.; Qi, H. H.; Tian, Y. J. *Appl. Phys. Lett.* **2005**, *87*, 123111.
(29) Koch, U.; Fojtik, A.; Weller H.; Henglein, A. *Chem. Phys. Lett.* **1985**, *122*, 507.
(30) Spanhel, L.; Anderson, M. A. *J. Am. Chem. Soc.* **1991**, *113*, 2826.
(31) Yang, R. D.; Tripathy, S.; Li, Y. T.; Sue, H. J. *Chem. Phys. Lett.* **2005**, *411*, 150.
(32) Harnack, O.; Pacholski, C.; Weller, H.; Yasuda, A.; Wessels, J. M. *Nano Lett.* **2003**, *3*, 1097.
(33) Li, Z. Q.; Xiong, Y. J.; Xie, Y. *Inorg. Chem.* **2003**, *42*, 8105.
(34) Liu B.; Zeng, H. C. *J. Am. Chem. Soc.* **2003**, *125*, 4430.